Tellus (1985), *37B*, 197–209

On radiative heating due to polar stratospheric clouds

By JEAN-PIERRE BLANCHET[1] *The International Meteorological Institute in Stockholm*[2], *Arrhenius Laboratory, S-10691 Stockholm, Sweden*

(Manuscript received February 8; in final form October 8, 1985)

ABSTRACT

Recent satellite observations of polar stratospheric clouds (PSCs) and the theoretical explanation of their formation brought up questions on the radiative effects of those thin clouds. Optical parameters are calculated for selected stages of the cloud development and for wavelengths between 1 and 40 μm. Radiative transfer calculations yield absolute values of heating rates of about 0.03 K/day for the thickest polar stratospheric clouds observed by the SAM II satellite. The top portion of the cloud is characterized by cooling of the order of 0.01 K/day while the lower and denser part of the cloud may experience either cooling or warming depending on the thermal structure and on the vertical distribution of clouds in the troposphere. Due to the correlation between cold stratosphere and warm troposphere, the radiative effect appears more sensitive to the distribution of cloud than to the strength of the surface temperature inversion. Unlike most tropospheric cases and under favorable conditions, the growth of cloud particles may reach equilibrium not only by depletion of ambient moisture but also by thermal equilibrium. The hypothetical fully developed cloud would lead to absolute values of the heating rates of the order of 1 K/day. The maximum warming is found in the wings of the 15 μm CO_2 band and extends up to 24 μm, while some cooling occurs at the upper end of the thermal spectrum. A simple parameterization of optical properties of PSCs is presented for inclusion into broad band radiation models.

1. Introduction

The temperature of the lower stratosphere is maintained by a balance between several diabatic and adiabatic heating and cooling processes. The adiabatic term is essentially due to vertical motion induced by a broad range of atmospheric waves from planetary scale so shorter gravity waves. The stable stratification results in hydrostatic force which dampens vertical motions. Typically horizontal heat advection is positively correlated with advection of moisture. Considering the low vapour pressure found in the stratosphere and the strength of cooling terms in that region, the supersaturation required to produce large scale clouds can be attained slowly. Near the polar tropopause in the lower stratosphere the relaxation time for radiative processes is of the order of 100 days. Conversely, the zonally averaged heating terms are typically much weaker (of the order of ± 0.1 K/day) than their tropospheric counterpart. Because of their magnitude and also because of measurement or model errors, it is often difficult to evaluate accurately individual contributions. The diabatic heat terms originate from a multitude of physical processes among which radiation occupies an important place in maintaining the thermal structure of the stratosphere. In the summer hemisphere, solar radiation absorbed around the tropopause tends to balance the emitted thermal radiation. Without solar heating at the winter pole the lower stratosphere temperature can become extremely low. Temperatures around 180 K have occasionally been observed near 15 km above Antarctica.

McCormick et al. (1982) reported extensive satellite observations showing formations of thin clouds in the polar stratosphere during winter. Most of those clouds are distinct from orographic clouds in that they are correlated with large scale minimum temperatures rather than with topo-

[1] *Permanent address:* Canadian Climate Centre, Downsview, Ontario, M3H 5T4, Canada.

[2] Contribution no. 532.

graphy. The polar stratospheric clouds (PSC) have a probability of occurrence exceeding 90% at temperatures below 185 K, while they become rare above 198 K. Those favorable conditions for PSC formations are much more frequent during winter over Antarctica than over Arctic regions.

Steele et al. (1983) explained the formation of PSCs from the condensation of water vapour on stratospheric aerosols in the Junge layer (10 to 25 km). This aerosol is thought to be composed essentially of concentrated (near 75%) sulphuric acid droplets (Toon and Pollack, 1973). When temperature decreases, the vapour pressure above the acid solution decreases and aerosol particles grow by molecular diffusion. Initially the equilibrium with ambient moisture is obtained by an increase of the water vapour pressure above droplet surfaces taking place when the acid solution is diluted. For highly diluted acid droplets this mechanism becomes inefficient and a rise of supersaturation eventually results in activation of the particles. Furthermore, the diluted and supercooled droplets are expected to freeze by homogeneous nucleation. The saturation vapour pressure is lowered to that characteristic of ice, resulting in an accelerated growth rate of the particles. Once nuclei are activated, growth progresses by condensation–deposition until an equilibrium is reached with available ambient moisture or until the temperature is raised to cancel the difference in vapour pressure between the particulate surfaces and the environment. In the initial stage of growth the increase in size of droplets is modest and the optical extinction coefficient increases slightly. During the second stage, activated nuclei drastically increase in size and the extinction coefficient also increases by one or two orders of magnitude. Steele et al. (1983) showed that these extinction coefficients are in excellent agreement with measurements from SAM II, providing good support for the cloud formation theory.

The change of temperature of the PSC layer is determined from a balance between emitted radiation away from the cloud and absorbed radiation coming from outside the cloud. The problem is analogous to the radiative transfer of heat between two grey bodies with different temperatures as ruled by Kirchhoff's law. Since PSCs are formed in the coldest region of the lower atmosphere (below the mesopause), heating is generally expected from upwelling thermal radiation at the cloud base. However, due to the exponential decrease of atmospheric opacity above cloud top, a cooling effect is expected at the top of PSCs. Obviously the net result depends on the temperature gradient above and below the cloud and on the opacity of the cloud.

With the increasing opacity of the PSCs, the upwelling infrared radiation originating from the warmer troposphere is absorbed by droplets or ice crystals much more efficiently than by water in its original vapour phase. Due to the low heat capacity of the sub-micron particles and the low density of the environment, relatively small radiation absorptions as compared to tropospheric counterparts are necessary to raise the temperature. Conversely, the local cooling rate is equally sensitive to the radiative emission by cloud particles. It is the purpose of this paper to investigate the perturbation of the radiative transfer resulting from the formation of PSCs. The results are relevant to climate modeling. It is a well known problem that general circulation models (GCMs) tend to produce abnormally low temperatures in the polar stratosphere. In turn the zonal wind component of the polar jet reaches unrealistic large values. The formation of PSCs appears as a mechanism that may physically alter this situation.

Very recently (after completion and review of the present work) a new paper by Pollack and McKay (1985) has shed some light on the problem of radiative effect of PSCs. Due to a fundamental difference in the conclusion regarding the sign of the resulting feedback, some extended calculations have been carried out in order to resolve this discrepancy.

2. Conditions and model

The paper is composed of three parts. First the optical properties of the PSCs are determined based on available observations and on the theory of clouds formation elaborated by Steele et al. (1983). Secondly, the optical parameters are included into a column radiation model of the atmosphere and spectral radiative heating is computed for observed and hypothetical conditions as predicted by the cloud formation theory. The effect of tropospheric temperature and cloudiness are also examined. Finally, a simple parameterization of the optical properties of PSCs is suggested for applications in climate modeling.

The minimum necessary optical parameters for radiation calculations, i.e. the volume extinction coefficient, the single scattering albedo and the asymmetry factor are computed from the Mie solution for spherical particles. The theoretical model of Steele et al. (1983) gives the size distribution and the composition of the aerosol as a function of the environmental temperature and for several water vapour mixing ratios. Using the background aerosol size distribution determined from extensive surveys by Rosen et al. (1975),

$$\frac{dN}{d\ln r} = \frac{N_0}{\sqrt{2\pi}\ln\sigma}\exp\left\{-\frac{1}{2}\left(\frac{\ln(r/r_g)}{\ln\sigma}\right)^2\right\} \qquad (1)$$

where $r_g = 0.0725$ μm is the mode radius and $\sigma = 1.86$, Steele et al. obtained remarkable agreement with direct observations for a mean aerosol concentration of $N_0 = 6$ cm^{-3}. The growth of particles with initial radii of 0.0725 and 0.29 μm as a function of temperature and for several water vapour mixing ratios is reproduced in Fig. 1 as given by Steele et al. (1983). The two initial sizes show the narrowing of the size distribution occurring during growth. Here only the case of 5 ppmv of water is considered, other cases being analogous. Their calculations of extinction coefficients at 1 μm result in a systematic increase of the extinction which essentially follows the evolution of the droplet size distribution.

As a consequence of diffusion growth theory, small particles grow relatively faster than larger ones and the size distribution narrows down during growth (Byers, 1965). Fig. 2 shows the relation of the standard deviation of the distribution as a function of the mode radius. This is evaluated from the change in the size of particles initially at 0.0725 and 0.29 μm (Fig. 1). The dots along the curve 5 ppmv in Figs. 1 and 2 indicate the cases where Mie calculations were performed for 50 wavelengths between 1.06 and 40 μm. Here it is implicitly assumed that the mode radius remains along the growth curve for the initial radius of 0.0725 μm. The spectral refractive index of sulphuric acid particles was interpolated from the results of Palmer and Williams (1975). In the limit of pure water, the refractive indices given by Hale and Querry (1973) were employed. No attempt has been made to use the refractive index for ice. Recent tests by Pollack and McKay (1985) show little sensitivity of the heating rate to the particle composition. Furthermore, the conditions of transition from water to ice are not known. In view of the uncertainties on particulate material density (0.6 to 0.9 g/cm^3) and crystal shape, the above constraint appears justified for the present estimation. The resulting volume extinction

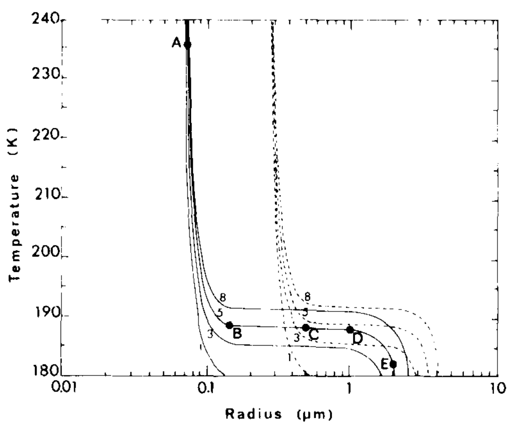

Fig. 1. Change of the droplet size with temperature for various water vapour mixing ratios (1, 3, 5 and 8 ppmv) at a pressure of 100 mb (adapted from Steele et al. (1983)). Two initial sizes are shown, 0.0725 (solid) and 0.29 μm (dashed). Particular points of interest (labeled A to E) are selected for extended Mie calculations in the 1 to 40 μm wavelength range.

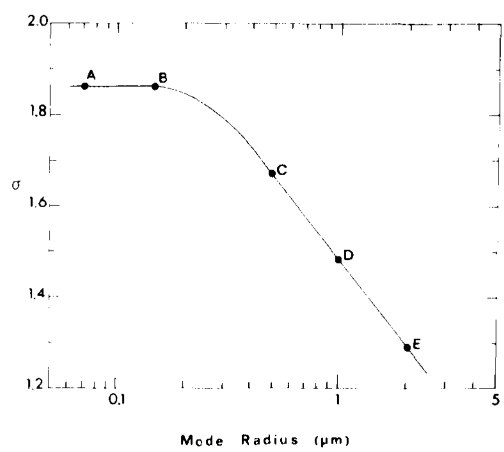

Fig. 2. Relation of σ with the mode radius as evaluated from Fig. 1. Values used in Mie calculations are labeled A to E.

coefficients and absorption coefficients are shown in Figs. 3 and 4 respectively.

The radiation model is based on the delta-Eddington method (Joseph et al., 1976) applied to thermal radiation in a plane parallel geometry. Thus the model accounts for multiple scattering to a reasonable degree of accuracy. Although scattering in the infrared is much smaller than in the visible, it is most significant for thin haze like PSCs, particularly for water vapour mixing ratios as low as 5 ppmv and in the weaker absorption regions of the near infrared. A total of 108 wavelengths intervals and 82 atmospheric layers constitute the calculation grid. Absorption by water vapour, carbon dioxide, ozone, nitric oxide, methane plus other less important trace gases are computed for AFGL data (Rothman, 1981) using a random band model (Malkmus, 1967). Details on the radiation model are presented in a separate paper (Blanchet and List, 1986).

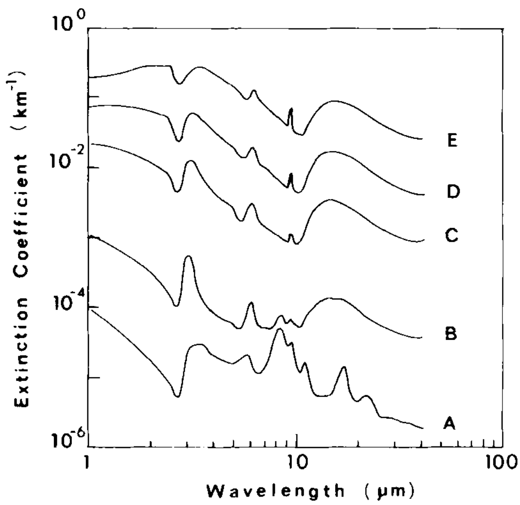

Fig. 3. Volume extinction coefficients for size distributions A to E in Figs. 1 and 2. The two bottom curves correspond to H_2SO_4 at 75% and 8.4%, respectively, while upper curves are assumed to be pure liquid water.

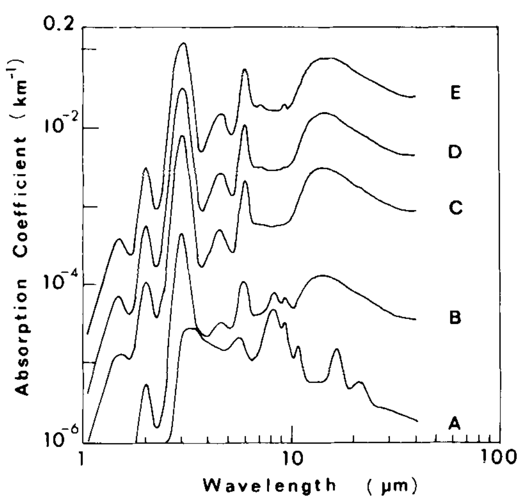

Fig. 4. As Fig. 3 but for spectral volume absorption coefficients.

Calculations are made for cases with and without aerosol. In each case the effect of aerosol is examined by subtracting results of the reference calculation from the results of the perturbed case, so the remainder is essentially due to aerosols.

3. Results and discussion

Satellite observations at 1 μm (SAM II) show that extinction coefficients exceeding 0.001 km^{-1} in the lower stratosphere are rather frequent for temperatures below 200 K. Although the actual measurements do not record extinction signals above 0.01 km^{-1}, it appears likely that higher extinction coefficients occur in extreme situations. In response to a temperature decrease, the theoretical model by Steele et al. (1983) predicts a rapid increase of the extinction coefficient up to about 0.1 km^{-1}. Further development of the hypothetical cloud leads to strong depletion of the ambient moisture such that PSCs could not exceed extinction coefficients larger than 1 km^{-1} at 1 μm.

The spectral extinction coefficients shown in Fig. 3 agrees with values obtained by Steele et al. (1983) at 1 μm (for $N_0 = 6$ cm^{-3}). Here those results are extended up to a wavelength of 40 μm for selected mode radii and correspondent size distribution width (Figs. 1 and 2). In Fig. 3, the lower curve represents background aerosol (75% H_2SO_4). The next curve shows the spectrum for highly diluted H_2SO_4 (8.4%). This spectrum has already acquired most characteristics of water drȯplets. At higher dilutions, the signature of H_2SO_4 vanishes. Fig. 4 shows the corresponding spectral absorption coefficients. Owing to the rapid increases of the efficiency factor for absorption with particles size and imaginary index of refraction at infrared wavelengths, the absorption increases from negligible values at 1 μm and progressively dominates the extinction at long wavelengths. In the 8 to 12 μm window, the computed single scattering albedo is in the vicinity of 50 to 60%, thus resulting in substantial scattering in the cloud.

At the scale of a single droplet and in the absence of other processes, the droplet temperature depends on the balance between absorbed and emitted radiation. Assuming that heat diffusion from contact with air molecules is capable of maintaining the droplet surface temperature in a close balance with the environmental temperature, then infrared radiative heating experienced by cold droplets in an upwelling radiation field from the much warmer troposphere is capable of heating the environment through heat conduction between droplets and their environment.

The macroscopic heating rate evaluated from infrared irradiance convergence in each model layers is computed for measured temperatures and extinction profiles obtained from SAM II data (McCormick et al., 1982, their figs. 8b and 8c) over Antarctica on July 28 and on September 1, 1979. At this stage, temperature, water mixing ratio and ozone amount are assumed to be those of the subarctic winter standard atmosphere (McClatchey et al., 1972) for the region of the atmosphere not given by McCormick et al. (1982). The tropospheric temperature is likely to be warmer than that typically encountered during PSC formation (Dieterichs, 1950) and consequently increases somewhat the upward irradiance at PSC heights. However, the first objective is to examine the effect of different stratospheric vertical distributions of PSC particles and the effect of particle growth during cloud formation. The effect of tropospheric, cloud and temperatures are examined separately in the next step. The net result for different profiles may be estimated from a composite effect of particulate distributions and temperature profile.

It must be emphasized that in the present study the secondary effect due to the reduction of specific humidity from condensed water vapour or precipitation are not considered. For submicron nuclei, those effects are negligible. They become considerable only for the largest particles found in the hypothetical mature stage of the clouds. In this work the attention is focused on some cases observed by SAM II and theoretical predictions by Steele et al. (1983) for the particle size.

The mid-range mode radius of 0.5 μm (Fig. 1) gives extinction corresponding to the peak value observed near 13 km on September 1. Fig. 5 shows the resulting heating rates. Maximum heating rates near 0.03 K/day are obtained for September 1 and much smaller values of the radiative heating are found for the case of July 28. Both cases give rise to cooling above the PSC due to reduction in upward irradiance from the lower troposphere and some radiative divergence in the top portion of the PSC. A weak "greenhouse" effect is seen in the troposphere from the warming trend. For the same particles size, Fig. 5 shows that the strongest local radiative effects of the cloud is achieved when the particles are most confined in the vertical direction and that a minimum extinction of the order of 0.01/km is required to produce substantial heating.

According to the theory presented by Steele et al. (1983), the development of a PSC occurs abruptly when the temperature decreases and aerosol particles are activated. In principle the particles could grow until equilibrium is reached with the available ambient moisture and produce extinction coefficients of the order of 0.1/km. In fact, most cases observed by SAM II lie in the low range of the

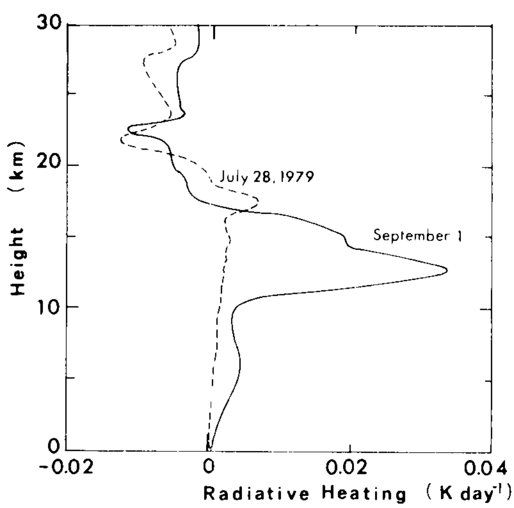

Fig. 5. Radiative heating perturbation due to polar stratospheric clouds. Two cases are shown: July 28 (dashed line) and September 1, 1979 (solid line), both events were observed by SAM II over the Antarctic region. The maximum extinction at 1 μm is, respectively, 0.002 and 0.02 km^{-1}. In both cases, a mode radius of 0.5 μm is assumed.

extinction values (β_e) and almost no "bunching" of the observed points (T, β_e) is found at the upper detection level of the SAM II instruments. In the event that the large scale extinction coefficient of PSCs would commonly exceed 0.01 km^{-1}, a large number of points would be found at the upper detection level. This suggests that the growth rate is very slow and a relatively stable equilibrium is reached much before the ambient moisture becomes strongly depleted (i.e. in the region B to C on Fig. 1).

Feedback processes leading to local heating represent another limiting process for the development of PSCs. For instance, the rapid increase of radiation convergence when droplets grow beyond point B gives rise to a temperature increase which alters the vapour pressure balance and can stop the condensation growth. This is seen when the size distribution is varied from B to E (Fig. 1) while keeping constant the vertical profile of the number density of particles. The result is shown in Fig. 6. The heating rate increases very rapidly to reach values exceeding 1 K/day. Under normal conditions encountered during large scale PSC formation, it is possible that a balance between cooling and heating terms occurs somewhere along the branch BD. This effect can explain the numerous observations of partly developed clouds (between B and C) reported by Steele et al. (1983). In that context the formation of a PSC appears to be a process capable of affecting the minimum temperature of the lower stratosphere. It is clear that the heating or cooling rate perturbation is extremely sensitive to the growth of particles at fixed number density.

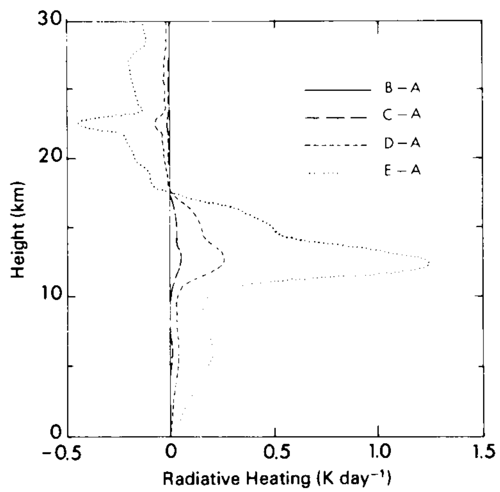

Fig. 6. Radiative heating perturbation resulting from theoretical values for PSCs droplet size. Here are shown the deviations from background aerosol (A) with a mode radius of 0.0725 μm. The mode radii for the perturbed cases are, respectively, (B) 0.15, (C) 0.5, (D) 1.0 and (E) 2.0 μm. In all cases, the particulate number density is fixed to the case of September 1 over Antarctica.

In the atmosphere, cloud particles are heated by release of latent heat of condensation (deposition) and in the present case by net convergence of radiation. Molecular heat diffusion is the remaining controlling process. Two limiting cases can reduce the cloud particle growth rate depending on the strength of molecular heat diffusion. First, in the limit of weak diffusion, the heating of particles would raise the superficial vapour pressure and reduce the particle growth. In this case the supersaturation of the environment would tend to increase when the ambient temperature is lowered. Secondly, if the heat diffusion process is sufficiently strong then the environmental temperature can increase through conduction and supersaturation decreases to reduce the growth rate of the cloud particles. For a single particle, the thermodynamic heat equation may be written as

$$\frac{dQ}{dt} = L\frac{dm}{dt} + \frac{1}{N_0}\frac{dF}{dz} - 4\pi fCK\delta T, \qquad (2)$$

where m is the mass of condensed water, F the net irradiance, z the height and δT the temperature difference between the particle and the environment. L, K and C refer, respectively, to the latent heat of sublimation, the thermal conductivity of the air and the shape factor (equal to the radius for spherical particles). f is an efficiency factor for heat conduction which includes effects of ventilation, kinetics of small particles and interactions with nearby sources and sinks. For small Reynolds and Prandtl numbers this correction is small and to a good approximation $f = 1$ (Miller and Young, 1979). Obviously to obtain a numerical solution, the growth equation is also needed together with interactive radiation. The microphysical processes involved in the cloud formation would need to be examined in detail in order to fully understand the formation of PSCs, but this objective is beyond the scope of the present work. However, from the above equation one can evaluate the importance of each term. This is shown in Table 1 for cases A to E of Fig. 1. Over a time scale of one hour, radiative heating is much larger than latent heat release and δT remains very small. Thus radiation is most likely to dominate the latent heat release during deposition and the temperature of the particles remains close to the ambient temperature.

Fig. 7 shows spectral radiative heating in the cloud layer (10 to 18 km) for September 1, 1979 with a mode radius of 0.5 μm. The integrated heating in each wavenumber interval of 25 cm^{-1} is plotted as a single horizontal bar. The cloud has a temperature between 181 and 195 K and consequently the Planck function is shifted toward longer wavelengths relative to that for tropospheric temperatures. Furthermore the reduction of the specific humidity increases the path length in the vicinity of 20 μm. As a result, maximum heating is obtained on both sides of the strong 15 μm CO_2 absorption band. Some heating originates from the lower troposphere (8 to 12 μm window) but a large portion of the contribution arises from radiative transfer of energy along a shorter path length between the middle or the upper troposphere and the PSC layer (12 to 24 μm). Small amounts of cooling are found in the rotation band (above 25 μm). In practise, this cooling balances the weak warming at shorter wavelengths (below 10 μm). As a result heating may be considered to take place effectively in the 10 to 24 μm wavelength interval. Pollack and McKay (1985) have shown that the cooling at very long wavelengths ($\lambda > 24$ μm) becomes more important in cases of extremely low tropospheric temperatures. A similar increase of cooling in the longwave range is expected for the case of extensive cirrus clouds underlaying the PSC layer (as discussed below).

Because of the extremely low temperature of

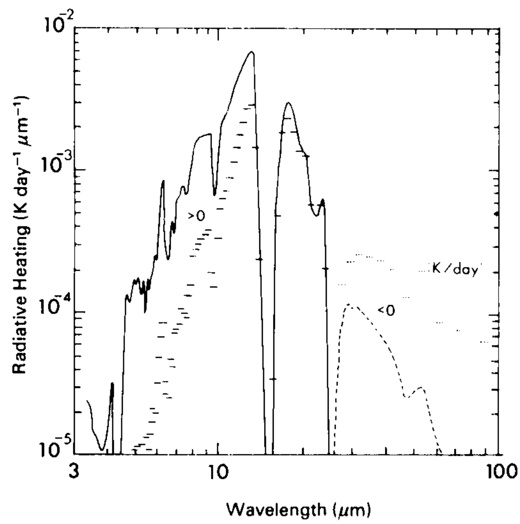

Fig. 7. Spectral radiative heating perturbation due to PSCs in the 10 to 18 km layer. Conditions are those of September 1, 1979 (Fig. 5) with the mode radius $r_g = 0.5$ μm. Solid lines represent warming and dashed lines are cooling. The short bars are the integrated heating rate (K/day) in each wavenumber interval of 25 cm^{-1}.

Table 1. *Comparison of heating/cooling terms for a single mean size particle*

	Radius (μm)	dQ/dt (rad) ($\times 10^{-7}$ W)	δT (K)	dQ (rad) ($\times 10^{-7}$ J)	dQ (dep) ($\times 10^{-7}$ J)
A	0.0725	0.000004	0.00002	0.013	
					0.0003
B	0.15	0.00001	0.00003	0.043	
					0.008
C	0.5	0.0003	0.0002	1.0	
					0.03
D	1.0	0.001	0.0005	3.7	
					0.2
E	2.0	0.007	0.001	25.0	

Columns are, respectively, from the left: (a) particle radius (μm), (2) radiative heating rate, (3) the temperature difference between the particle and the environment due to a balance between radiation and molecular diffusion, (4) radiative heating per article per hour and (5) the heating due to latent heat of deposition.

PSCs, the greenhouse effect is enhanced. The calculated perturbation of the upward irradiance at the top of the atmosphere and attributed to the formation of PSCs (September 1, 1979) is shown in Fig. 8 together with the integrated contribution of each spectral interval. As opposed to clouds and aerosols in the lower troposphere, this perturbation is not limited to the 8 to 12 μm window region (e.g. Blanchet and List, 1986) but covers the whole spectrum. A maximum is reached around a wavelength of 20 μm. Despite the relatively low optical depth, the presence of PSCs alters considerably the total irradiance at the top of the atmosphere (Fig. 9).

All the calculations above were performed using a standard subarctic temperature profile in the lower troposphere. This choice represents an upper limit of the temperature, of upwelling radiation at the PSC base and consequently an upper limit of the radiative heating in PSCs. Since October 1978 (McCormick et al., 1981), a long series of observations of the extinction coefficient indicates that PSCs often occur when an extremely cold stratosphere is associated with an abnormally warm troposphere. This negative correlation of the stratospheric and tropospheric temperatures favours the heating effect of PSCs. Further, PSCs are often associated with a strong meridional flow in the troposphere characteristic of blocking situations. In the Northern Hemisphere, these blocking flows are much more common due to the ocean-land thermal contrast and to the topography. Consequently, the temperature of the Northern Arctic stratosphere rarely reaches the level required for the formation of PSCs.

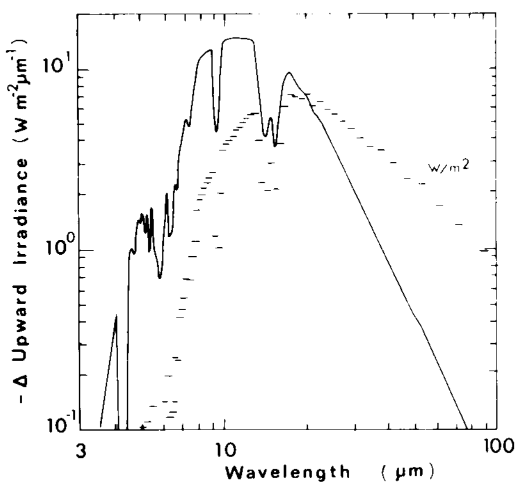

Fig. 8. Spectral upward irradiance perturbation at the top of the model due to PSCs (September 1, 1979 and r_g = 0.5 μm). A decrease of irradiance is seen at all wavelengths. The short bars are the integrated irradiance in each wavenumber interval of 25 cm^{-1}. Maximum values are reached at about 20 μm.

Typical synoptic situation of PSCs occurrence show a mid-tropospheric trough to the west of PSC formations, thus a poleward flow of warm and moist air in the troposphere. This situation normally results in extensive tropospheric cloud formations. For these reasons the effect of tropospheric temperature and clouds on PSCs must be further examined.

Pollack and McKay (1985) also examined the effect of PSCs for the observed stratospheric conditions of September 1, 1979. Their standard calculation corresponds to the extreme minimum temperature observed over the high antarctic plateau at any particular height. Geographically, the present calculations correspond to cases above low surfaces near sea level. Using the ECMWF FGGE 3B grid temperatures, it is found that on September 1, 1979 the minimum stratospheric temperature (associated with PSCs) occurred in the southern part of the Weddell Sea, near Berkner Island. In fact, ground observations show a high frequency of stratospheric clouds in the sector of the Weddell Sea (Stanford, 1977) and Ross Sea

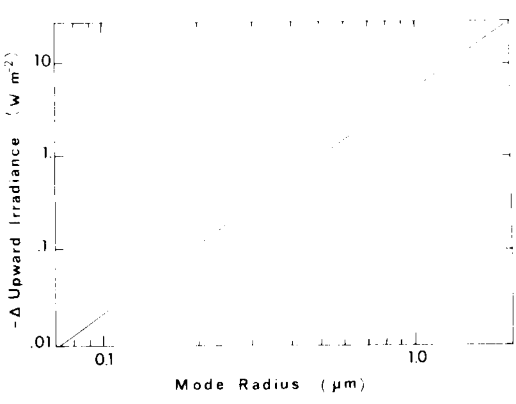

Fig. 9. Total upward irradiance decreases at the top of the model due to PSCs (September 1) as a function of mode radius of the cloud droplets distribution.

near Victoria Island (Hamill and McMaster, 1984). The 100 mb height analysis shows a cold low centered on Lesser Antarctica with a trough extending toward south America. Correspondingly, a pronounced warm ridge was established near 30W over the coast of Weddell Sea. The tropospheric temperature near Berkner island was above normal (Table 2).

For intercomparison purposes, the heating rate perturbation was calculated with the same PSC characteristics of Fig. 5 for September 1 but using the atmospheric temperature of the standard case given by Pollack and McKay (1985) with a surface temperature of 195 K at 680 mb. Fig. 10 shows cooling everywhere in the stratosphere and a weak tropospheric warming. At the PSC mass center (150 mb), the perturbation has a similar amplitude to the corresponding case in Fig. 5 for the warm troposphere (subarctic standard atmosphere) but of opposite sign. This result is in agreement with the result of Pollack and McKay (1985). It is of interest to notice that the lower stratosphere is most affected by the tropospheric temperature. The upper portion of aerosol (above 50 mb) is affected slightly by this modification.

A more realistic case is considered by using the FGGE 3B temperature data for that particular event (Table 2). The results are shown in Fig. 11 for two different surface temperature inversions. The main portion of the PSC layer is warmed much less than in the case of the standard sub-Arctic trosposphere. Once again the upper region (above 50 mb) is practically unaffected. Similar calculations for particle size which have reached the mature stage of the PCS development (D to E in Figs. 1 and 2, and a ground temperature of 230 K) indicate that the heating rate perturbation is increased in the same proportion as shown in Figs. 5 and 6, and the potential effect at full PSC development under these conditions is about 0.6 K/day.

Finally, the effect of underlying tropospheric cloud layers is investigated. Using the FGGE 3B temperature profile, two extreme cloud types are assumed: (1) a stratus layer with a top at 888 mb and a temperature of 249.2 K, and (2) a cirrus

Table 2. *Atmospheric temperature profiles used in the present work*

Troposphere				Stratosphere	
Pressure (mb)	Subarctic winter	FGGE 3b 1/Sept/79	Extremely cold	Pressure (mb)	All cases (*)
1013.0	257.1	230.0	—	241.8	203.0
887.8	259.1	249.2	—	206.6	195.0
777.5	255.9	245.8	—	176.6	191.0
679.8	252.7	242.3	195.0	151.0	190.0
600.0			223.0	129.1	188.0
515.8	240.9	233.8		110.3	186.0
500.0			221.0	80.6	183.0
446.7	234.1	227.9	215.0	68.8	181.0
385.3	227.3	222.0	209.0	58.8	182.0
330.8	220.6	216.3	202.0	50.1	184.0
282.9	211.0	207.1	195.0	31.1	194.0
241.8	203.0	203.0	203.0	22.6	206.0
206.7	195.0	195.0	195.0	10.2	216.0
176.6	191.0	191.0	191.0	2.2	234.7
151.0	190.0	190.0	190.0	0.57	259.3
				0.04	245.7

The subarctic winter atmosphere is taken from McClatchey et al. (1972) while the extremely cold troposphere is mostly based on the standard case of Pollack and McKay (1985). In the stratosphere, only the case corresponding to September 1, 1979 is shown. The last column (*) represents all cases except the one with cirrus where the cloud surface at 206.6 mb is assumed to have a temperature of 198.5 K.

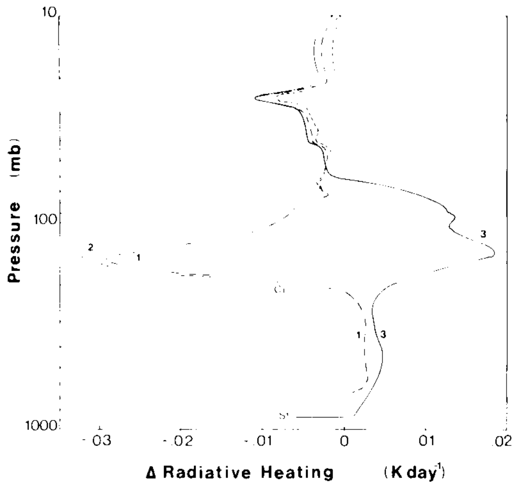

Fig. 10. As Fig. 5 but for the case of September 1 only and different tropospheric conditions. Curve 1 (long-dashes—dots) represents the heating rate perturbation for extremely cold temperatures over the Antarctic plateau as from the standard case of Pollack and McKay (1985). Curves 2 (dashed) and 3 (solid), respectively for cirrus and stratus, show the effect of tropospheric clouds on the heating perturbation. Curve 2 and 3 are based on observed FGGE 3B temperature data over southern Weddell Sea where the minimum stratospheric temperature occurred on that particular day.

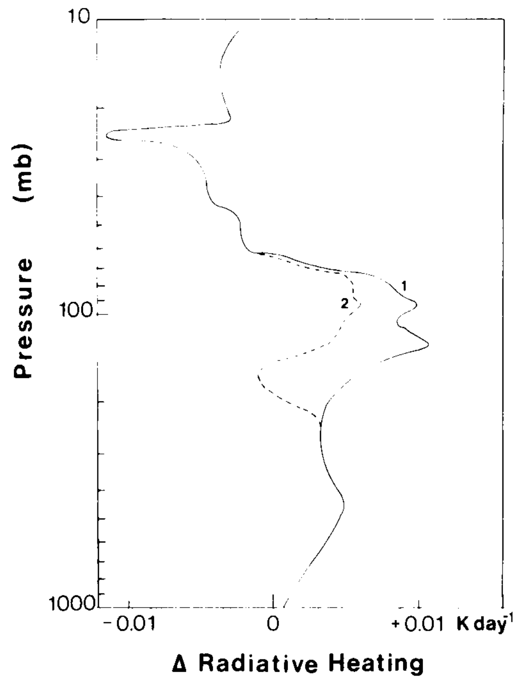

Fig. 11. As Fig. 10 but for a clear troposphere and FGGE 3B temperature profile. The effect of the surface temperature inversion is shown by imposing a ground temperature of 230 K (solid line 1) and 210 K (dashed line 2). A linear temperature gradient is assumed between the ground and 600 m where the temperature is 242° K.

layer up to 207 mb with a top temperature of 198.5 K. Both clouds are assumed to be radiative black bodies. The results are shown in Fig. 10. In agreement with above results, the perturbation at the PSC mass center fluctuates strongly with the characteristic temperature of the upwelling radiation. Since the tropospheric cloud condition is likely to vary with a much greater amplitude than the tropospheric temperature itself, then those clouds appear to be the controlling factor that determine the sign of the PSC radiative heating rate. In the case where PSCs are formed in the poleward flow to the east of a cold trough, the warm and moist troposphere most likely contains extensive vertical cloud formations. This synoptic condition would favour the cooling of the PSC layer and enhance the PSC formation (positive feedback). In that case, the presence of PSCs acts to vertically propagate the tropospheric cloud formation into the lower stratosphere. It must be kept in mind that, in the winter polar atmosphere, the tropopause is poorly defined and often PSCs may be regarded as high tropospheric clouds. On the other hand, if the PSCs extend over a warm ridge where extensive low stratus are common then the presence of PSCs would act to heat the lower stratosphere and limit the development of PSCs (negative feedback).

Because of this radiative interaction between the troposphere and the stratosphere, the net large scale effect of PSCs can only be determined from diagnostic analysis of grid data from observations or from general circulation model (GCM) simulation. Obviously the GCM must have a reliable interactive cloud parameterization. At the present stage, the treatment of tropospheric cloud is one of the problems in GCMs. However, the parameterization of PSCs appears to be simpler and an elementary model of PSCs optical properties may be considered.

A parameterization of the PSCs effect can be made on the basis of above results. In some respects PSCs are much simpler than any tropospheric clouds. The reasons are the relatively well-defined characteristics of the condensation nuclei in the stratosphere and the narrow range of possible water vapour mixing ratios. For these reasons the formation of PSCs is very well correlated with temperature and water vapour mixing ratio. In a radiation model based on the integral form of the transfer equation (Schwarzchild's equation), the effect of scattering is ignored and the emissivity in the appropriate wavelength intervals is calculated from the absorption coefficient at any given temperature and water vapour mixing ratio. Since the aerosol has only negligible radiative effect in the region A to B (Fig. 1), the background aerosol extinction may be considered constant at a minimum background value $\bar{\beta}_{min}$ (Fig. 12). The effect of increasing the water vapour mixing ratio, shown by Steele et al. (1983), results in cloud development occurring at a higher temperature and also in a potentially larger maximum particle size.

The broad-band transmission is given by

$$\bar{t} = e^{-\bar{\tau}/\bar{\mu}} \tag{3}$$

where $\bar{\mu} = 0.6$, the effective broad band optical thickness $\bar{\tau}$ is

$$\bar{\tau} = \int \bar{\beta} N(z)\, dz \tag{4}$$

$\bar{\beta}$ is an attenuation coefficient at 100 mb, z is the height and $N(z)$ is the normalized particulate number density in the Junge layer with respect to

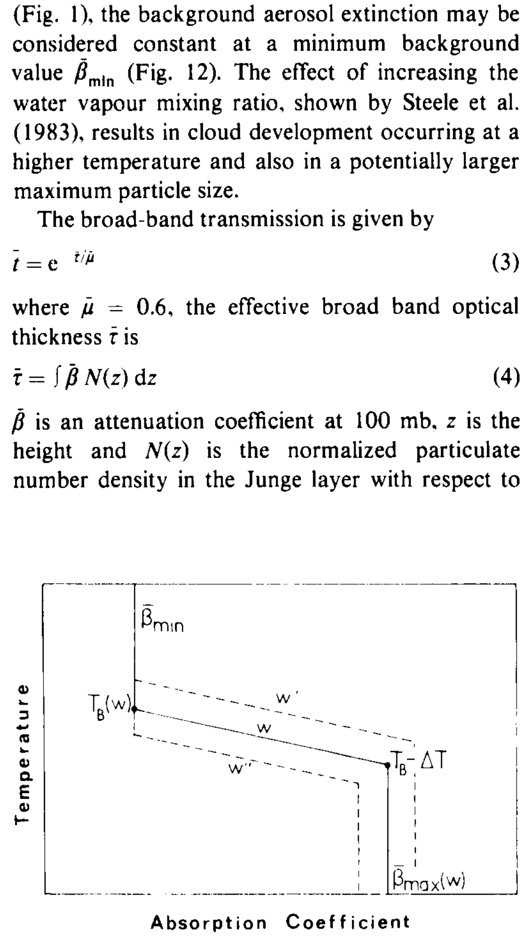

Fig. 12. Schematic representation of the broad band parameterization (10 to 25 μm) of the absorption coefficient as a function of temperature and water vapour mixing ratio.

the number density at 100 mb (6 cm^{-3}). The common assumption in parametrized thermal radiation models is to ignore scattering. In that case the attenuation is approximated by the mean absorption coefficient (km^{-1}) in the 10 to 24 μm interval (Fig. 12)

$$\bar{\beta}_a(T, w) = \begin{cases} \bar{\beta}_{min}, & T \geqslant T_B(w) \\ \min\,(10^{\gamma}, \bar{\beta}_{max}(w)), & T < T_B(w) \end{cases} \tag{5}$$

where

$$\gamma(T, w) = \frac{T - T_B(w)}{\Delta T} \log_{10}\left(\frac{\bar{\beta}_{min}}{\bar{\beta}_{max}(w)}\right) + \log_{10} \bar{\beta}_{min},$$

and

$$\bar{\beta}_{min} = 8 \times 10^{-6}\ \mathrm{km}^{-1},$$

$$\bar{\beta}_{max}(w) = 0.0063\, w + 0.018,$$

$$T_B(w) = 179.4\, w^{0.0313} + T_c$$

$$T_c = \frac{\Delta T}{2} - 1,$$

where T is the local temperature (K) and w the water vapour amount (ppmv). γ is the slope of $\log_{10}(\bar{\beta})$ versus temperature T in the transition region between B and D. ΔT can be evaluated from the result of Steele et al. (1983). A value of ΔT = 2 K appears adequate for this scheme. However, as can be inferred from Fig. 1, in the event of negative feedback, the formation process may not be properly resolved by a GCM with coarse vertical resolution and large radiation time steps (i.e., the PSCs would then oscillate as a switch between $\bar{\beta}_{min}$ and $\bar{\beta}_{max}$ extreme conditions). In this case a larger ΔT transition may be assumed in order to allow the model to establish a temperature equilibrium in the range B to D (Fig. 1). The term T_c is added as a correction term for ΔT larger than 2 K. More elaborate parameterization schemes may be obtained from detailed results, however, for most GCM applications this simple empirical formula appears adequate. It should be emphasized that this approach is only applicable in the limit that particulate temperatures are equal the environmental temperature.

4. Summary

The radiative heating resulting from PSCs has been examined by use of Mie calculations for spherical particles and a narrow band radiation model. The spectral irradiance convergence is maximum in the wings of the 15 μm CO_2 band and covers mostly the region between 10 and 24 μm. The integrated results indicate heating rates of the order of ± 0.03 K/day for a case corresponding to the maximum extinction coefficients (at 1 μm) observable by SAM II. However, the theoretical development of PSCs results in potentially larger opacity. The predicted heating of a fully developed cloud is shown to be near ± 1 K/day. The sign of the perturbation is essentially determined by the characteristic temperature of the upwelling thermal radiation. For extremely cold clear troposphere the radiative effect of PSCs is a positive feedback in agreement to results of Pollack and McKay (1985). However, due to the negative correlation between stratospheric and tropospheric temperatures for the particular case investigated, the heating is expected to dominate in the denser PSC layer. Since this local heating rate is capable of balancing the cooling process that produces the PSC, it is possible that PSC development may be limited by radiative heating rather than by available water vapour. In these circumstances, a PSC would develop to the point where a thermal equilibrium is reached. The heating rate perturbation is most strongly affected by tropospheric cloud conditions. High-level cirrus result in maximum cooling (positive feedback) while low stratus lead to maximum heating (negative feedback). These results imply that the formation of PSCs can substantially affect the temperature of the lower stratosphere. Because of the radiative coupling between the troposphere and the stratosphere together with the high sensitivity of the feedback in the PSC formation process to the particular synoptic conditions, the large scale effect of PSCs must be assessed from large scale observational data or from GCM simulations. The above results are relevant to GCMs since those models often generate excessively low temperatures in the lower polar stratosphere causing strong stratospheric zonal circulation. A simple parameterization is suggested to include the effect of PSCs in broad band radiation codes.

5. Acknowledgements

The author wishes to thank Drs. H. Sundqvist, J. Heintzenberg and B. Ritter for valuable comments on the present work. This study was supported by the Canadian Climate Centre and the International Meteorological Institute in Stockholm.

REFERENCES

Blanchet, J.-P. and List, R. 1986. Radiative effects of anthropogenic aerosol components in Arctic haze and snow: Results from a surface-atmosphere coupled model. *Tellus 38B*, in press.

Byers, H. C. 1965. *Elements of cloud physics*. University of Chicago Press, 191 pp.

Dieterichs, H. 1950. Über die Entstehung der Perlmutterwolken. *Meteorol. Rundsch. 3*, 208–213.

Hale, G. M. and Querry, M. R. 1973. Optical constants of water, the 200-nm to 200 μm wavelength region. *Appl. Opt. 12*, 555–563.

Hamill, P. and McMaster, L. R. 1984. Polar stratospheric clouds: their role in atmospheric processes. Proceedings of a Workshop held in Virginia Beach, Virginia, June 20–22, 1983. NASA Conference Publication 2318. 72p.

Joseph, J. H., Wiscombe, W. J. and Weinman, J. A. 1976. The delta-Eddington approximation for radiative flux transfer. *J. Atmos. Sci. 33*, 2452–2459.

Malkmus, W. 1967. Random Lorentz band model with exponential-tailed S^{-1} line-intensity distribution function. *J. Opt. Soc. Am. 57*, 323–329.

McClatchey, R. A., Fenn, R. W., Selby, J. E. A., Volz, F. E. and Garing, J. S. 1972. Optical properties of the atmosphere. AFCRL-72-0497. Environmental Research papers, No. 411. 108 pp.

McCormick, M. P. and Brandl, D. 1981. SAM II measurements of the polar stratospheric aerosol. Volume 1. October 1978 to April 1979. NASA Ref. Pub. 1081, Vol. 1, 78p.

McCormick, M. P., Steele, H. M., Hamill, P., Chu, W. P. and Swissler, T. J. 1982. Polar stratospheric cloud sightings by SAM II. *J. Atmos. Sci. 39*, 1387–1397.

Miller, T. L. and Young, K. C. 1979. A numerical simulation of ice crystal growth from the vapour phase. *J. Atmos. Sci. 36*, 458–469.

Palmer, K. F. and Williams, D. 1975. Optical constants of sulfuric acid; application to the clouds of Venus? *Appl. Opt. 14*, 208–219.

Pollack, J. B. and McKay, C. P. 1985. The impact of polar stratospheric clouds on the heating rates of the winter polar stratosphere. *J. Atmos. Sci. 42*, 245–262.

Rosen, J. M., Hoffmann, D. J. and Laby, J. 1975. Stratospheric aerosol measurements II: The worldwide distribution. *J. Atmos. Sci. 32*, 1457–1462.

Rothman, L. S. 1981. AFGL atmospheric absorption line parameters compilation: 1980 version. *Appl. Opt. 20*, 791–795.

Stanford, J. L. 1977. On the nature of persistent stratospheric clouds in the Antarctic. *Tellus 29*, 530–534.

Steele, H. M., Hamill, P., McCormick, M. P. and Swissler, T. J. 1983. The formation of polar stratospheric clouds. *J. Atmos. Sci. 40*, 2055–2067.

Toon, O. B. and Pollack, J. B. 1973. Physical properties of the stratospheric aerosols. *J. Geoph. Res. 78*, 7051–7056.